

Enhanced Corrosion Resistance of AZ91D Magnesium Alloy by Electric Field – Assisted Anodizing

Xinjian Song, Yujun Si*, Jin Liu, Minjiao Li, Zhongping Xiong

College of Chemistry and Environmental Engineering, Sichuan University of Science and Engineering, Zigong, 643000, China

*E-mail: syj08448@163.com

Received: 22 April 2019 / Accepted: 12 June 2019 / Published: 31 July 2019

An external electric field was imposed on electrolytic cell in anodization of AZ91D magnesium alloy. The anodizing process became more stable with the assistance of the external electric field, and the obtained anodization film was smoother and compact. As a result, the corrosion resistance of the anodization film was enhanced. The external electric field can drive the anions in the electrolyte, especially the citrate ion with more negative charge and larger volume, to migrate to the surface of the AZ91D electrode to form the anodization film. The greatest carbon content could be obtained at an 8 V of external electric field, which corresponded to the best microstructure and corrosion resistance of the anodization film.

Keywords: Magnesium alloy; Anodizing; External electric field; Ionic motion; Corrosion resistance

1. INTRODUCTION

Magnesium alloys are widely used as structural materials in transportation industries due to the low density and high strength to weight ratio. The energy consumption and emission of hazardous substances can be reduced by decreasing the mass of transportation tools. However, magnesium is active with a standard potential of -2.37 V (vs. SHE). It is prone to be corroded and deteriorate the strength of magnesium alloys parts [1-4]. Alloying magnesium with other elements is an effective way to weaken the activities of magnesium alloys. For example, Mg-9Al-1Zn alloy (AZ91) shows high corrosion resistance in typical corrosion media [5, 6]. AZ91D alloy has a microstructure with two phases, a matrix of α -grains with β phase (intermetallic $Mg_{17}Al_{12}$). The β phase mainly serves as a cathode and accelerates the corrosion of the α -matrix if the volume fraction of β phase is small. However the β phase may act as an anodic barrier to inhibit the overall corrosion of the alloy for a high fraction [7-9].

Surface treatment is another method to further improve the anti-corrosion ability of magnesium

alloy, including chemical conversion treatments [10], electrochemical anodization [11,12], electroless plating [13,14], organic-polymer deposition [15], plasma electrolytic oxidation (PEO) [16,17], and laser surface alloying [18, 19], etc. Among these methods, electrochemical anodization is widely studied due to the good hardness, adhesion, abrasion resistance and anti-corrosion ability of the anodization film. HEA and DOW17 are the successful anodization processes [20, 21]. But their applications are still restrained because of the electrolytes containing environmentally harmful fluoride or chromate. Developing environmental friendly electrolyte has been the research topic in the anodization of magnesium alloys [22-24].

In this work, AZ91D alloy was anodized in a green electrolyte containing silicate, citrate and borate. To obtain a compact anodization film with better corrosion resistance, an external electric field was creatively imposed on the electrolytic cell during the anodization process. The migration of ions in the electrolyte were tuned with the assistance of the external electric field, and the resulted anodization film showed better anti-corrosion performance.

2. EXPERIMENTAL

A 5 mm-thick round AZ91D specimen was cut from a rod with a diameter of 20 mm (cross-section area is 3.14 cm²). The specimen was connected with a copper wire and embedded in epoxy resin leaving one side exposed as working surface. The working surface was polished with SiC emery paper up to 1200 grid, and rinsed with deionized water prior to anodizing.

The anodization electrolyte (250 mL) contained 50 g/L NaOH, 40 g/L Na₂B₄O₇·10H₂O, 60 g/L Na₂SiO₃·9H₂O, and 20 g/L C₆H₅Na₃O₇·2H₂O (sodium citrate). Anodization was carried out at a current density of 10 mA cm⁻² for 20 minutes at 25 °C by using a stainless steel sheet as counter electrode.

To tune the migration of ions in the electrolyte, an external electric field was imposed on the electrolytic cell by putting two stainless steel sheets outside the electrolytic cell during anodizing. As illustrated in Fig. 1, AZ91D alloy and stainless steel sheet I in the electrolyte were connected to the positive and negative electrode of the a DC power source for anodizing, respectively. The positive electrode of a second DC power source was connected to the stainless steel sheet II near the AZ91D electrode to provide an external electric field. According to the theory about ionic mobility, the migration of anions in the electrolyte solution to the surface of AZ91D anode could be changed with the assistance of the external electric field [25]. As a result, the composition and property of the anodization film will be tuned. The effect of the external electric field was investigated at the voltages of 0 V, 4V, 8 V, 12 V and 16 V.

The morphology of the anodization film on AZ91D was observed using scanning electron microscopy (SEM, VEGA 3 EasyProbe, TESCAN). The composition of the film was measured by an energy dispersive X-ray spectrometer (EDS, Bruker). The phase structure of the film was identified using X-ray diffractometer (XRD, DX-2600, Dandong Fangyuan) with Cu K α radiation at a scanning rate of 5 ° min⁻¹. The thickness of film was tested by a coating thickness gauge (DR 380, Guangzhou Dongru).

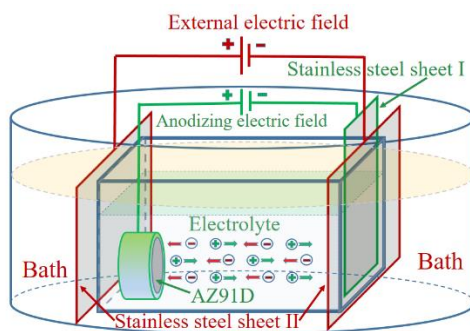


Figure 1. Electrolytic cell for anodizing with an external electric field.

The corrosion resistance of the anodization film was evaluated by electrochemical open circuit potential (OCP) and electrochemical impedance spectrum (EIS) tested on a CHI760E (Chenghua) electrochemical workstation in 3.5 wt% NaCl solution at 25 °C. The anodized AZ91D, a saturated calomel electrode (SCE) and a platinum sheet were used as the working, reference and counter electrodes, respectively. The OCP was first collected and then the EIS test was carried out at the OCP over the frequency range from 10^5 Hz to 0.1 Hz with a perturbation of 5 mV.

3. RESULTS AND DISCUSSION

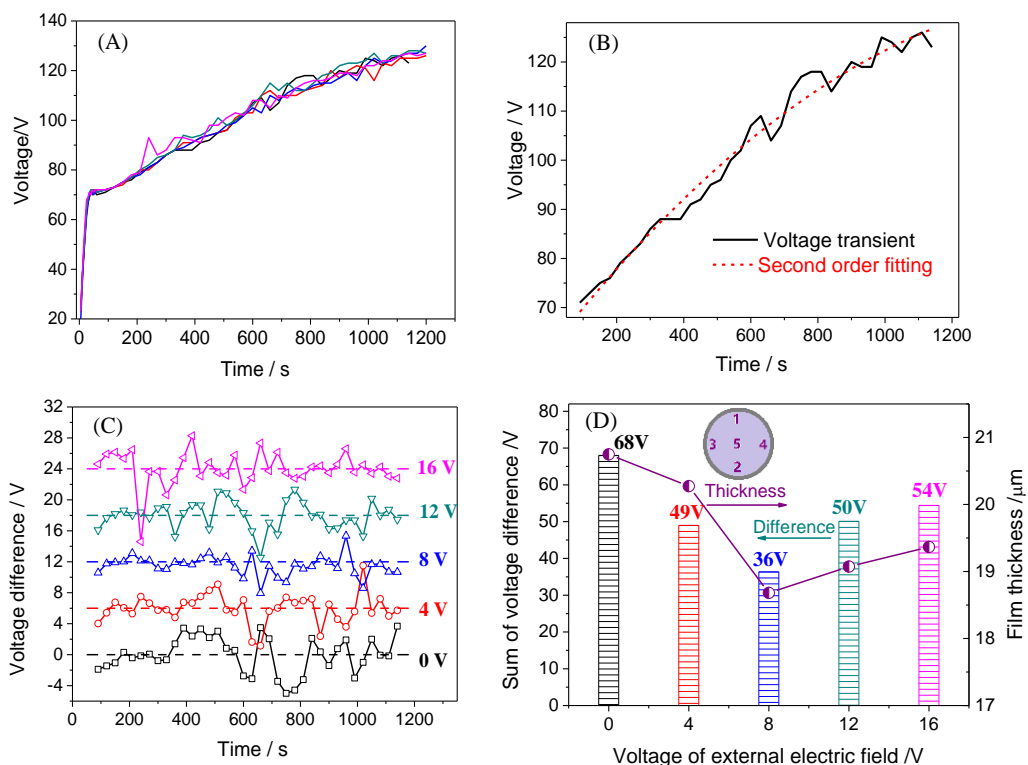


Figure 2. (A) Voltage transients of the anodizing processes at different external electric fields, (B) the fitting of voltage transient at 0 V of external electric field, (C) the voltage differences between the experimental data and the fitted results, (D) the sum of the absolute values of voltage differences (column graph) and average thickness of anodization film (line graph).

The voltage of the anodizing electric field was recorded during the experiment. Fig. 2(A) shows the voltage transients with the assistance of an external electric field of 0 V, 4 V, 8 V, 12 V and 16 V. Once the anodizing current is supplied, the cell voltage immediately rises up to about 70 V because of the formation of insulated anodization film. After anodized for about 40 s, the voltage increases slowly and dispersed faint sparks occur on the anode surface. The spark becomes bigger with the increase of film thickness, but the quantity of spark decreases. The voltage also violently fluctuates at the end stage of the anodizing.

Different voltage fluctuations were observed at different voltage of external electric field. To evaluate the fluctuation, the voltage transient from 90 s to 1200 s was fitted by a polynomial function with second order as shown in Fig. 2(B). The voltage difference between the experimental data and the fitted results was calculated and shown in Fig. 2(C). Fig. 2(D) shows the sum of the absolute values of the voltage differences. The smaller difference sum corresponds to the stable anodizing and better integrity of the anodization film. The thickness of anodization film was tested three times at five positions on the electrode. The average thicknesses of five specimens were also shown in Fig.2(D).

It can be observed that the voltage of the anodizing electric field dramatically fluctuates without the assistance of the external electric field (at 0 V). Then the voltage becomes stable by applying an external electric field of 4 V on the electrolytic cell. The sum of the absolute value of the voltage difference reduces from 68 V of 0 V to 49 V of 4 V, and further decreases to 36 V of 8 V. A good relativity between the film thickness and voltage difference can also be found. Thinner anodization film can be obtained in a more stable anodizing with smaller voltage difference. These results reveal that the external electric field can promote the formation of compact anodization film. The anodization voltage becomes unstable again, and the sum of the absolute value of the voltage difference increases to 50 V of 12V and to 54 V of 16 V of external electric field. It was observed that the stainless steel sheet II dissolved at the higher voltages and the bath became muddy. The side reaction on the stainless steel II at higher voltage makes the effect of the external electric field complicated.

Fig. 3 displays the XRD patterns of the anodization film of AZ91D alloy obtained at different second fields and the enlarged pattern of the anodized film formed at a second electric field of 8V. The strong diffraction peaks of α -Mg phase (PDF 35-0821) and the weak diffraction peaks of β - $\text{Al}_{12}\text{Mg}_{17}$ phase (PDF 01-1128) can be checked out. The other diffraction peaks correspond to MgO (PDF 45-0946), MgSiO_3 (PDF 19-0768), MgB_2O_6 (PDF 38-1475) as shown in Fig. 3(B).

The XRD measurements show that the silicate and borate ions take part in the formation of the anodized films and exist as MgSiO_3 and MgB_2O_6 , respectively. The material containing carbon cannot be checked out in the XRD patterns, meaning carbon element exists as amorphous phase in the anodization film. The intensities of the diffraction peaks of MgO are strengthened with the second electric field. Comparing to the greater fluctuation of anodization voltage at 16 as shown in Fig. 2, the excessive MgO is harmful to form uniformed anodization film.

Fig. 4 shows the Nyquist curves and Bode plots for the anodization films of AZ91D. The Nyquist curves obtained at an external electric field of 0 V and 4 V are composed of two capacitive semi-circles at high and low frequency regions. The two capacitive semi-circles tend to merge as a big semi-circle with increasing the external electric field to 8 V, 12 V and 16 V. The pronounced increase in the impedance (Fig. 4(B)) indicates a significant improvement in corrosion resistance. As expected, the

anodization film of 8 V has the largest impedance among all the samples, confirming that this sample has the highest corrosion resistance.

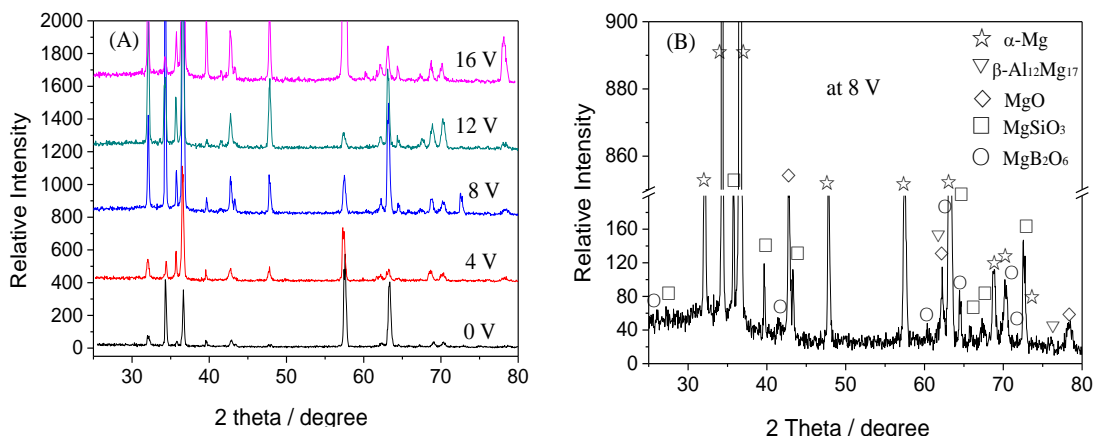


Figure 3. XRD patterns of anodization films on AZ91D substrate formed at different external electric fields, (A) full patterns and (B) enlarged pattern of the film obtained at an external electric field of 8 V.

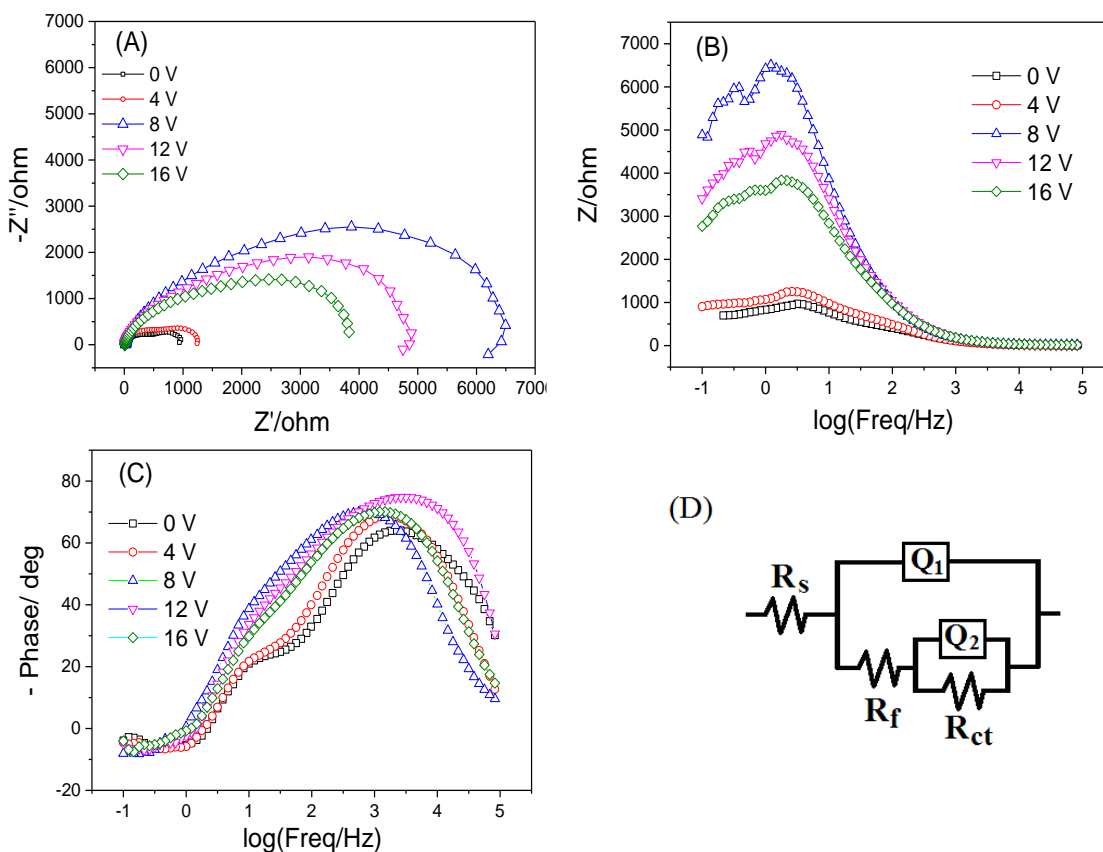


Figure 4. EIS spectra of anodization film of AZ91D obtained at different voltages of external electric field in 3.5 wt% NaCl solution. (A) Nyquist curves, (B) Bode plots of Z vs. frequency, (C) Bode plots of phase angle vs. frequency, (D) equivalent circuit model.

Based on the Bode plots of phase angle vs. frequency shown in Fig. 4(C), the impedance spectra can be fitted by an equivalent circuit model with two time constants by ZSimpWin Software as shown in Fig. 4(D). In the equivalent circuit, R_s is the resistance between the reference and working electrodes; R_f is the resistance of anodization film; Q_1 is the constant phase element (CPE) in anodization film; R_{ct} is the charge transfer resistance at substrate/anodization film interface; Q_2 is the double-layer CPE in substrate/anodization film interface. The greater R_f and R_{ct} mean that the anodization film is compact and the charge transfer is difficult in the anodic dissolution of magnesium.

The relation of R_f and R_{ct} with the voltage of external electric fields was presented in Fig. 5(A). Obviously, both the two resistances increased by applying an external electric field on the electrolytic cell in the anodizing process. The greatest R_f and R_{ct} can be obtained at 8 V, which corresponds to the thinnest film and the best corrosion resistance of the anodization film. The result is consistent to the open circuit potential, the sum of voltage difference in anodizing process as shown in Fig. 5(B), in which the -1.55 V of open circuit potential of anodization film obtained at 8 V of the external electric field is the most positive. The minimal 18.68 μm of film thickness and the smallest sum of voltage difference of 36 V of anodization film obtained at 8 V means the film is more compact, which is the origin of the better anti-corrosion ability.

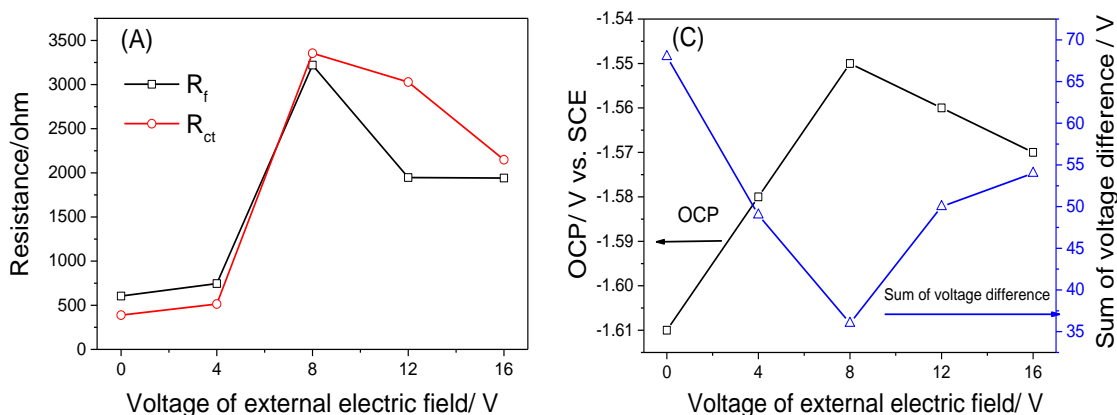


Figure 5. (A) Relation between R_f and R_{ct} with the voltage of external electric field, (B) relation between OCP and sum of absolute value of voltage difference with the voltage of external electric field.

Fig. 6 presents the morphologies of the anodization films obtained at different voltages of external electric field. The quantity and diameter of micro-pore in the anodization film decrease with the assistance of an external electric field from 4 V to 8 V, and the anodization film is smoother and compact. Then the compactness of the anodization film deteriorates by increasing the voltage of the external electric field to 12 V and 16 V. Correspondingly, the corrosion resistance of the anodization film also deteriorates as shown in Fig. 5. Comparing to some typical references [22, 23, 26-29], the anodization film obtained in this work is more compact and uniform. Especially the anodization film obtained at an external electric field of 8 V has less and smaller micro-pore. The compact structure of the anodization film is the origin of the enhanced corrosion resistance.

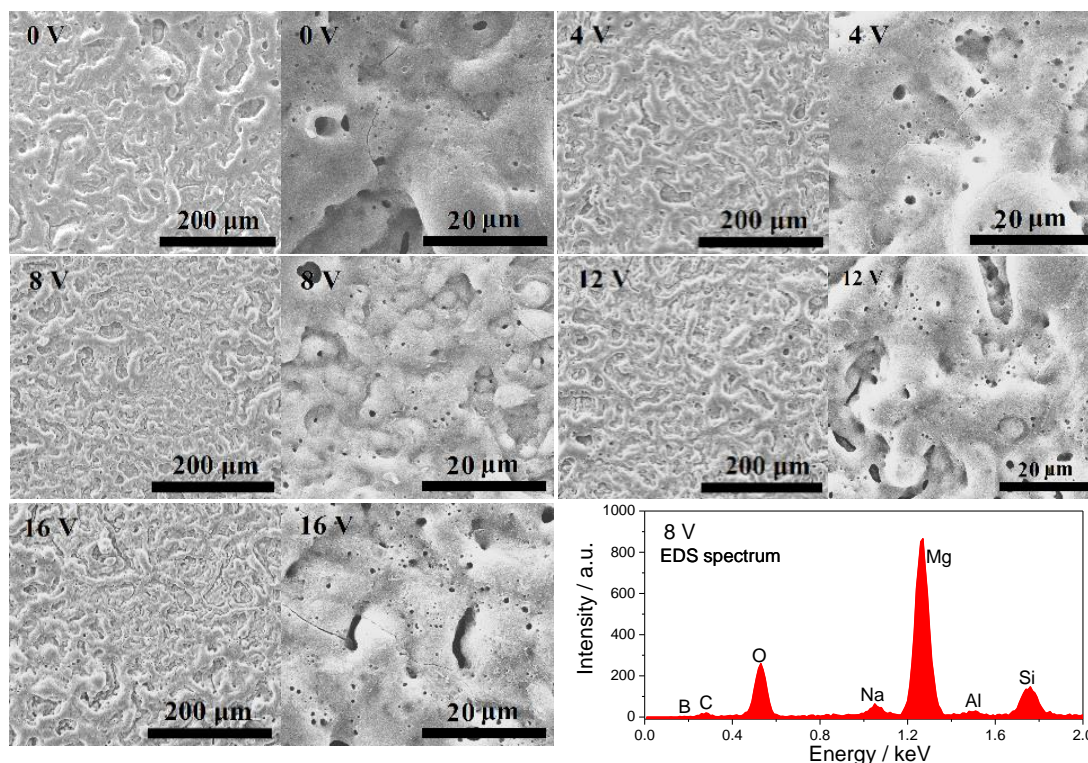


Figure 6. Morphologies of anodization films of AZ91D at two magnitudes and EDS spectrum of anodization film obtained at 8 V of external electric field.

The EDS spectrum of the anodization film obtained at 8 V of external electric field was also shown in Fig. 6. The atom contents of magnesium, oxygen, boron, carbon and silicon elements were shown in Fig. 7. The magnesium and oxygen are the dominant elements in the anodization film. No obvious relationship can be concluded between the content of magnesium and the voltage of the external electric field. The content of oxygen decreases from 39.09 at% to 35.27 at% and 34.1 % by increasing the voltage of external electric field from 0 V to 4 V and 8 V, then increases to 40.37 at% and 40.66 at% for 12 V and 16 V of external electric field. The content change of oxygen is similar to the change of sum of voltage difference as shown in Fig. 2, so the lower content of oxygen is beneficial to obtain compact anodization film.

The boron, silicon and carbon atoms existing as anions in the electrolyte, their contents do not simply increase with the voltage of the external electric field. The content of boron gradually decreases from 8.87 at% to 4.81 at% with changing the voltage of the external electric field from 0 V to 16 V. The content of silicon keeps about 8 at% and no obvious relation with the anti-corrosion resistance of anodization film.

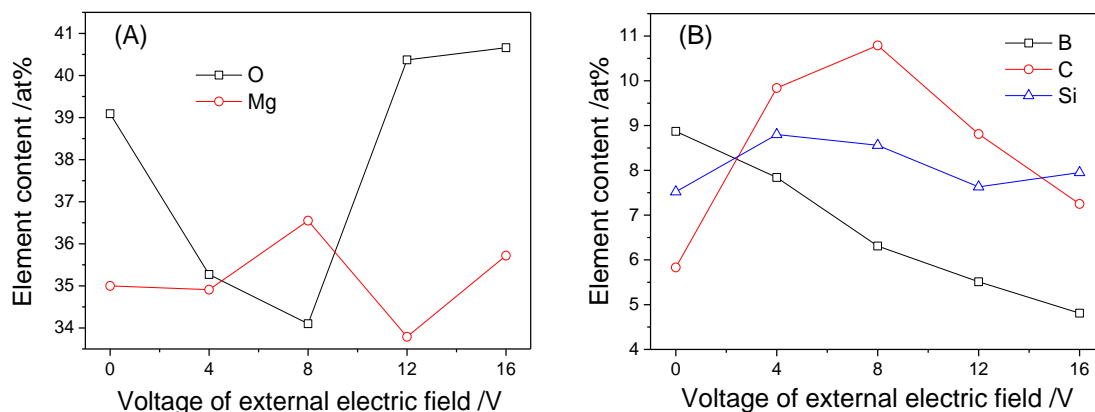


Figure 7. Atom contents of the anodization films obtained at different voltages of external electric field.

It is noted that the content of carbon increased from 5.83 at% to 9.84 at% and 10.79 at% by increasing the voltage of external electric field from 0 V to 4 V and 8 V, then decreases to 8.81 at% and 7.25 at% for 12 V and 16 V. The content change of carbon is similar to the change of corrosion resistance as shown in Fig. 4. It is safe to deduce that the effect of the external electric field is to tune the relative content of elements in the anodization film. The greatest content of carbon and lowest oxygen content can be obtained at 8 V of external electric field, which corresponds to thinnest film and the best anti-corrosion ability of the anodization film of AZ91D alloy. So the carbon element plays important role to the formation of compact anodization film.

According to the above results, the possible mechanism for the improvement in corrosion resistance of AZ91D anodization film is schematically proposed in Fig. 8. The Mg dissolves as Mg^{2+} in the anodizing process and the anions in the electrolyte solution migrate to the surface of AZ91D electrode. Among the anions, hydroxide ions, borate ions and silicate ions combine with Mg^{2+} to form MgO , MgB_2O_6 and $MgSiO_3$ as the main components of the anodization film, respectively. But the citrate ions were absorbed on the anodization film, and then were carbonized to small fragments by electric sparks with high temperature. These fragments fill up the flaws and decrease the quantity and diameter of the micro-pores in the anodization film. So the existence of the carbon fragment is beneficial to form compact film and enhance the corrosion resistance of the anodization film [30, 31]. Although the migration of all anions can be accelerated by the external electric field in the anodizing process of AZ91D, the citrate ion is more sensitive because of its more negative charge and larger volume. So the

flaws in anodization film can be more effectively filled and the anodization film shows better integrity and corrosion resistance with greater carbon content.

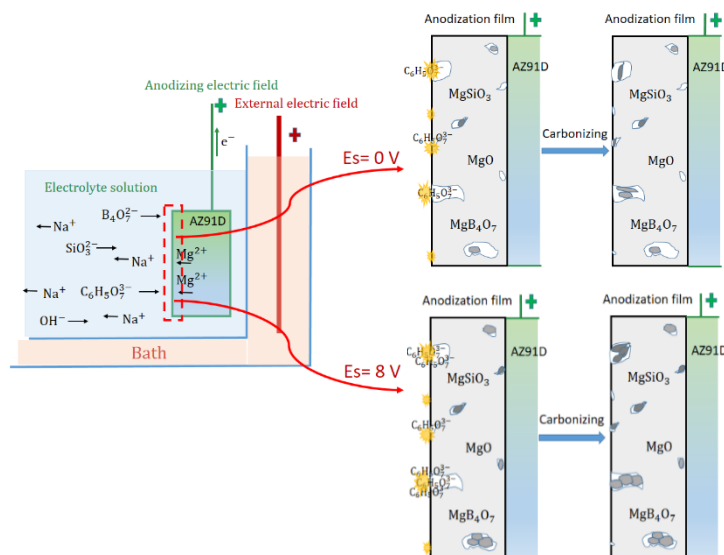


Figure 8. Schematic representation of the effect of the external electric field in the anodizing process of AZ91D alloy.

4. CONCLUSIONS

An external electric field was imposed on electrolytic cell to tune the migration of ions in the anodization of AZ91D alloy. The absolute value of the anodizing voltage difference between experimental data and fitted results is 68 V, 49 V, 36 V, 50 V and 54 V with the assistance of an external electric field of 0 V, 4 V, 8 V, 12 V and 16 V, respectively. A stable anodizing process with smallest voltage difference of 36 V and uniformed anodization film with minimal film thickness of 18.68 μm was obtained at 8 V. The application of external electric field increases the content of carbon in anodization film. The maximum carbon content of 10.79 at % was obtained at 8 V of external electric field. Citrate ion is more sensitive to the external electric field than hydroxide ion, borate ion and silicate ion. That is the reason why the content of carbon in anodization film increases with the voltage of the external electric field from 0 V to 8 V. Smaller quantity and small micro-pores were observed in the anodization film obtained at 8 V and the film is smoothest and compact. The film resistance and electron transfer resistance is also the biggest. The corrosion resistance of anodization film can be enhanced with the assistance of the external electric field of 8 V.

ACKNOWLEDGEMENTS

This work was supported by the Sichuan Science and Technology Program (2019YJ0458), the Opening Project of Sichuan Key Laboratory of Comprehensive Utilization of Vanadium and Titanium Resources (2018FTSZ05), and the Opening Project of Key Laboratory of Green Catalysis of Sichuan Institutes of High Education (No. LZJ18201).

References

1. F. Cao, G.L. Song and A. Atrens, *Corros. Sci.*, 111 (2016) 835.

2. X.J. Wang, D.K. Xu, R.Z. Wu, X.B. Chen, Q.M. Peng, L. Jin, Y.C. Xin, Z.Q. Zhang, Y. Liu, X.H. Chen, G. Chen, K.K. Deng and H.Y. Wang, *J. Mater. Sci. Technol.*, 34 (2018)245.
3. S. Kumar and S.K. Das, *J. Alloys Compd.*, 740 (2018) 626.
4. Y. Si, Z. Xiong, X. Zheng, M. Li and Q. Yang, *Int. J. Electrochem. Sci.*, 11(2016) 3261.
5. Z. Shi, G.L. Song and A. Atrens, *Corros. Sci.*, 47 (2005) 2760.
6. J.H. Jun, *J. Alloys Compd.*, 725 (2017) 237.
7. G.L. Song, A. Atrens, X.L. Wu and B. Zhang, *Corros. Sci.*, 40(1998) 1769.
8. H.Y. Choi and W.J. Kim, *J. Alloys Compd.*, 696 (2017) 736.
9. W. Li, W. Li, L. Zhu, H. Liu and X. Wang, *Mat. Sci. Eng. B*, 178 (2013) 417.
10. G.P. Abatti, A.T.N. Pires, A. Spinelli, N. Scharnagl and T.F. da Conceicao, *J. Alloys Compd.*, 738 (2018) 224.
11. Z. Shi, G.L. Song and A. Atrens, *Corros. Sci.*, 48 (2006) 1939.
12. A.D.F. Lopez, I.L. Lehr and S.B. Saidman, *J. Alloys Compd.*, 702 (2017) 338.
13. Z. Rajabalizadeh and D. Seifzadeh, *Appl. Surf. Sci.*, 422 (2017) 696.
14. M. Heshmati, D. Seifzadeh, P. Shoghi and M. Gholizadeh-Gheshlagh, *Surf. Coat. Tech.*, 328 (2017) 20.
15. M.A. Surmeneva, A. Vladescu, C.M. Cotrut, A.I. Tyurin, T.S. Pirozhkova, I.A. Shuvarin, B. Elkin, C. Oehr and R.A. Surmenev, *Appl. Surf. Sci.*, 427 (2018) 617.
16. W. Tu, Y. Cheng, X. Wang, T. Zhan and J. Han, Y. Cheng, *J. Alloys Compd.*, 725 (2017) 199.
17. D. Chen, R. Wang, Z. Huang, Y. Wu, Y. Zhang, G. Wu, D. Li, C. Guo, G. Jiang, S. Yu, D. Shen and P. Nash, *Appl. Surf. Sci.*, 434 (2018) 326.
18. L.X. Chen, Y. Liu, Z.Y. Liu, X.Y. Zhao and W. Li, *Mat. Corrosion*, 66 (2015) 963.
19. C. Meng, Z. Chen, G. Li and P. Dong, *J. Alloys Compd.*, 711 (2017) 258.
20. H.A. Evangelides, U.S. Pat. 2723952,1955.11.15.
21. C.C.Dow, G.B. Pat. 762195,1956.11.28.
22. Y. Liu, Z. Wei, F. Yang and Z. Zhang, *J. Alloy. Compd.*, 509 (2011) 6440.
23. A. Yabuki and M. Sakai, *Corros. Sci.*, 51 (2009) 793.
24. G.L. Song and Z. Shi, *Corros. Sci.*, 85 (2014) 126.
25. A. Bard and L. Folkner, *Electrochemical methods: Principles and applications*, New York: Wiley, 2001.
26. X. Wang, L. Zhu, W. Li, H. Liu and Y. Li, *Appl. Surf. Sci.*, 55 (2009) 5721.
27. L. Chai, X. Yu, Z. Yang, Y. Wang and M. Okido, *Corros. Sci.*, 50 (2008) 3274.
28. X. Guo, M. An, P. Yang, H. Li and C. Su, *J. Alloys Compd.*, 482 (2009) 487.
29. X. Lu, X. Feng, Y. Zuo, P. Zhang and C. Zheng, *Prog. Org. Coat.*, 104 (2017) 188.
30. J. Zhao, X. Xie and C. Zhang, *Corros. Sci.*, 114 (2017) 146.
31. Q. Tan, A. Atrens, N. Mo and M.X. Zhang, *Corros. Sci.*, 112 (2016) 734.